INFECTION AND IMMUNITY, May 2001, p. 3398–3409 Vol. 69, No. 5
0019-9567/01/$04.00+0 DOI: 10.1128/IAI.69.5.3398–3409.2001

Molecular Basis for Immunoglobulin M Specificity to Epitopes in *Cryptococcus neoformans* Polysaccharide That Elicit Protective and Nonprotective Antibodies

ANTONIO NAKOUZI,[1] PHILIPPE VALADON,[2] JOSHUA NOSANCHUK,[1] NANCY GREEN,[3] AND ARTURO CASADEVALL[1,4]*

Division of Infectious Diseases, Department of Medicine,[1] and Departments of Pediatrics[3] and Microbiology and Immunology,[4] Albert Einstein College of Medicine, Bronx, New York 10461, and Sidney Kimmel Cancer Center, San Diego, California 92121[2]

Received 22 December 2000/Returned for modification 24 January 2001/Accepted 7 February 2001

The protective efficacy of antibodies (Abs) to *Cryptococcus neoformans* glucuronoxylomannan (GXM) is dependent on Ab fine specificity. Two clonally related immunoglobulin M monoclonal Abs (MAbs) (12A1 and 13F1) differ in fine specificity and protective efficacy, presumably due to variable (V)-region sequence differences resulting from somatic mutations. MAb 12A1 is protective and produces annular immunofluorescence (IF) on serotype D *C. neoformans,* while MAb 13F1 is not protective and produces punctate IF. To determine the Ab molecular determinants responsible for the IF pattern, site-directed mutagenesis of the MAb 12A1 heavy-chain V region (V_H) was followed by serological and functional studies of the various mutants. Changing two selected amino acids in the 12A1 V_H binding cavity to the corresponding residues in the 13F1 V_H altered the IF pattern from annular to punctate, reduced opsonic efficacy, and abolished recognition by an anti-idiotypic Ab. Analysis of the binding of the various mutants to peptide mimetics revealed that different amino acids were responsible for GXM binding and peptide specificity. The results suggest that V-region motifs associated with annular binding and opsonic activity may be predictive of Ab efficacy against *C. neoformans*. This has important implications for immunotherapy and vaccine design that are reinforced by the finding that GXM and peptide reactivities are determined by different amino acid residues.

The protective efficacy of antibodies (Abs) to the human-pathogenic fungus *Cryptococcus neoformans* depends on the Ab isotype and specificity (reviewed in references 3 and 46). The evidence that Ab specificity is critical for protective efficacy comes from studies of two clonally related immunoglobulin M (IgM) monoclonal Abs (MAbs) known as 12A1 and 13F1 (3, 31, 39, 46). Although these MAbs originated from the same B-cell precursor and use the same variable (V)-region genes, they differ in specificity as a result of V-region somatic mutations that translate into 12 amino acid differences (31, 39). The differences in specificity are manifested by differences in the indirect immunofluorescence (IF) binding pattern such that MAbs 12A1 and 13F1 produce annular and punctate patterns, respectively, after binding to serotype D *C. neoformans* cells (11, 31, 39). The annular binding pattern is correlated with opsonic efficacy, capsular reaction patterns, and complement activation kinetics (27) and Ab protection against serotype D organisms (31, 39). Since the MAb pair 12A1 and 13F1 have markedly different biological properties yet differ in sequence by only a few amino acids, they provide a unique opportunity for the study of Ab specificity.

MAbs to *C. neoformans* capsular glucuronoxylomannan (GXM) have been grouped into five classes based on V-region usage and idiotype and serotype specificity (5). Class II MAbs include a large set of MAbs that bind to an immunodominant epitope found in all cryptococcal serotypes and are characterized by the use of V_H7183, J_H2, V_κ5.1, and J_κ1 gene elements and a heavy-chain V (V_H) third complementarity-determining region (CDR3) of 11 amino acids (5). MAbs 12A1 and 13F1 are class II MAbs (5). Peptide mimetics which bind to the antigen (Ag) binding sites of class II MAbs have been described (43, 44), and the crystal structures of the class II MAb 2H1 with and without a complexed peptide mimetic have been solved (47). Murine class II MAbs and human Abs to *C. neoformans* GXM share sequence similarities (40). The class II MAb 18B7 is in clinical evaluation for the treatment of cryptococcal meningitis (4).

IgM is an important isotype against fungi in light of evidence that some IgMs are protective against *C. neoformans* (17, 32) and *Candida albicans* (20), and IgM is common in both the human and mouse responses to GXM (6, 16, 22). IgM may have an advantage over IgG in therapy because it is very effective at clearing Ag but does not elicit lethal toxicity reactions when administered to *C. neoformans*-infected mice (26). Identification of the amino acid residues that confer Ab specificity for epitopes associated with protection is important for defining the Ab paratope, or the site that is involved in binding the polysaccharide Ag (19), and the latter is important for immunotherapy and vaccine design. In this study, we used site-directed mutagenesis to identify the amino acids responsible for the fine-specificity difference between MAbs 12A1 and 13F1 and compared the serological and opsonic properties of the mutated Abs. The fact that punctate and annular IF patterns reflect differential localization of Ag-Ab complexes on the *C. neoformans* capsule (15) indicates that the binding char-

* Corresponding author. Mailing address: Division of Infectious Diseases, Department of Medicine, Albert Einstein College of Medicine, 1300 Morris Park Ave., Bronx, NY 10461. Phone: (718) 430-3665. Fax: (718) 430-8701. E-mail: casadeva@aecom.yu.edu.

acteristics of IgM may require valence or other structural constraints. Therefore, we changed the 12A1 V_H to the corresponding residue in the 13F1 V_H and expressed the mutated V regions. The results indicate that annular binding is conferred by two V_H amino acid residues that impart major differences in biological function by coding for two different epitope specificities.

MATERIALS AND METHODS

Hybridomas and MAbs. Hybridomas 12A1 and 13F1 both produce IgM MAbs (6). Cells were maintained in Dulbecco modified Eagle (DME) medium containing 10% fetal calf serum (Harlan, Indianapolis, Ind.), 10% NCTC-109 (Mediatech, Herndon, Va.), and 1% nonessential amino acid solution (Mediatech). MAb 3E5 is an IgG3 which competes with MAb 12A1 but not 13F1 (31).

Heavy-chain-nonproducing hybridoma mutants. The 12A1 heavy-chain-nonproducing hybridoma cells were isolated by soft agar cloning followed by overlaying the agar with rabbit antiserum to murine IgM. In this method, colonies that secrete IgM are stained by Ag-Ab precipitates. Colonies that were not stained were selected and transferred to 96-well plates containing cell medium, and their supernatants were tested for IgM and light-chain κ secretion by enzyme-linked immunosorbent assay (ELISA) (see below). Hybridoma cells that tested negative for IgM and positive for light-chain κ were used in the transfection experiments.

***C. neoformans* and other yeasts.** Serotype D strain 24067 was obtained from the American Type Culture Collection (Manassas, Va.). MAbs 12A1 and 13F1 produce annular and punctate IF patterns, respectively, upon binding to the 24067 capsule. *C. neoformans* cells were maintained in glycerol stocks at −80°C and grown in Sabouraud dextrose broth (Difco Laboratories, Detroit, Mich.) for 24 h at 30°C with constant shaking at 150 rpm. Before use, cells were washed three times with sterile phosphate-buffered saline (PBS) and counted using a hemacytometer. Capsular GXM was prepared from supernatants of strain 24067 as described previously (9). *Saccharomyces cerevisiae* strain 1H170 *his3 ade2* and *C. albicans* strain SC5314 were gifts from Lorraine Marsh (Bronx, N.Y.) and Mahmoud Ghannoum (Cleveland, Ohio), respectively.

V_H and V_L sequences. Total RNA was isolated from hybridoma cells using Trizol reagent (Gibco BRL, Gaithersburg, Md.). cDNA was generated using reverse transcriptase and the oligonucleotide primer p(dt)15 (Boehringer Mannheim, Indianapolis, Ind.). DNA containing the V_H region was amplified using the primers 5′-TAAAAAGCTTAGTC CACTCGCCATGGACTTC-3′ and 5′-T ATATTGCTAGCTGAGGAGACTGTGAGAGTGG-3′. DNA containing the light-chain V region (V_L) was amplified using the primers GATGTTGTGATG ACCCAA and TGGATGGTGGGAAGATG. The amplified DNA was cloned into the PCR 2.1 vector (Invitrogen, San Diego, Calif.) for sequencing. Oligonucleotide synthesis and DNA sequencing were done by the Oligonucleotide Facility of the Cancer Center at Albert Einstein College of Medicine.

Expression of 12A1 V_H. DNA containing MAb 12A1 V_H was excised from the PCR 2.1 vector using *Nhe*I and *Hin*dIII (Promega, Madison, Wis.) and cloned into a murine cDNA IgM expression vector (28). The plasmid was then transfected into heavy-chain-nonproducing 12A1 hybridoma cells by electroporation using conditions of 200 Ω, 960 μF, and 450 V. The same recipient cell line deficient in heavy-chain production was used to generate all mutant Abs. Approximately 3×10^6 cells were washed with cold PBS, mixed with 10 to 15 μg of plasmid in 1.0 ml of PBS, placed in a Gene Pulser cuvette (Bio-Rad Laboratories, Hercules, Calif.), and incubated on ice for 10 min before transfection. Following electroporation, cells were incubated on ice for 10 min and then washed with DME medium. Cells were then plated at a density of 10^4 cells/well in a 96-well plate (Becton Dickinson Labware, Franklin Lakes, N.J.) for 24 h in feeding medium. Cells expressing the transfected plasmid were selected with 1.5 mg of neomycin (Geneticin; Gibco BRL)/ml in DME medium with 20% fetal calf serum (Harlan), 10% NCTC-109 (Mediatech), and 1% nonessential amino acid solution (Mediatech). To identify high-producing clones, the cells were cloned in soft agar with an overlay of rabbit Ab to mouse IgM. Colonies with strong Ag-Ab staining were selected. Transfected cells produced 10 to 150 ng of IgM/ml in cell culture supernatants after 24 h of incubation.

Site-directed mutagenesis. Amino acid changes were introduced into the MAb 12A1 V_H by oligonucleotide-directed PCR mutagenesis using a QuickChange site-directed mutagenesis kit (Stratagene, La Jolla, Calif.). The oligonucleotides (5′→3′) for mutagenesis were as follows: N31S, GCCTCTGGATTTACTTCCA GTAGCTATTTCATGTCTTGGG and CCCAAGACATGAAATAGCTACTG AAAGTGAATCCACAGGC; F33Y, CACTTTCAGTAACTATTACATGTCT TGGG and CCCAAGACATGTAATAGTTACTGAAAGTG; M50A, GAG GCTGGAATTGGTCGGAGCCATTAATATTAATGGTGATAACACC and GGTGTTATCACCATTAATATTAATGGCTGCGACCAATTCCAGCC TC; I53S, GGCTGGAATTGGTCGCAATGATTAATAGTAATGGTGATAA CACCTAC and TATCCGGATAGTAGGTGTTATCACCATTACTATTAAT CATTGCGACCAATTCCAGCC; N56G, GGTCGCAATGATTAATATTAAT GGTGGTAACACCTACTATCCA and GTCTGGATAGTAGGTGTTACCA CCATTAATATTAATCATTGCGACC; N57S, ATTAATGGTGATAGCACC TACTATCCAGAC and GTCTGGATAGTAGGTGCTATCACCATTAAT; D80Y, GCCAAGAACACCCTGTACCTGCAAATGAGCAGTCTG and CAC ACTGCTCATTTGCAGGTACAGGGTGTTCTTGGC; and G103Y, GCAAG ACGAGACGGCACCTACGGAAACTACTTTGACTAC and GTAGTCAA AGTAGTTTCCGTAGGTGCCGTCTCGTCTTGC. The oligonucleotide primers, each complementary to opposite strands of the vector, extend during temperature cycling by means of *Pfu* DNA polymerase. On incorporation of the oligonucleotide primers, a mutated plasmid containing staggered nicks is generated. Following temperature cycling, the PCR product was treated with *Dpn*I, an endonuclease specific for methylated and hemimethylated DNAs that digests the parental DNA template and selects for molecules containing the mutation. The DNA was then used to transform *Escherichia coli* supercompetent cells and make purified DNA for electroporation experiments. Despite multiple attempts, we were not able to generate a 12A1 variant expressing the G103Y mutation. All mutations were confirmed by sequence analysis.

ELISAs. Ab concentrations were determined by ELISA. Polystyrene plates were coated with goat anti-mouse IgM, blocked with 1% bovine serum albumin (BSA) in PBS, and incubated with the IgM-containing solution. Bound IgM was detected using alkaline phosphatase-conjugated goat anti-mouse IgM, and the IgM concentration was determined relative to isotype-matched IgM standards (Southern Biotechnology, Birmingham, Ala.). IgM binding to GXM was studied by ELISA as described previously (7). Briefly, polystyrene plates were coated with a GXM solution (1 μg/ml) and blocked with 1% BSA in PBS. IgM-containing solutions were then added, and bound IgM was detected using alkaline phosphatase-conjugated goat anti-mouse IgM. Competition ELISAs were done to determine whether MAb 3E5 (IgG3) could inhibit the binding of the mutagenized MAb 12A1 derivatives to GXM as described previously (31). For this ELISA, variable amounts of the Ab in question were mixed with a constant amount of MAb 3E5 (2 μg/ml) and allowed to react with GXM absorbed on a polystyrene plate. Binding of IgG3 was detected by isotype-specific alkaline phosphatase-conjugated goat anti-mouse reagents. Reactivity with the anti-idiotypic MAb 7B8 was also measured by ELISA. Briefly, plates were coated with 1 μg of goat anti-mouse IgM/ml, blocked with 1% BSA in PBS, incubated with the IgM MAb, and then incubated with MAb 7B8 (IgG1), and binding was detected with goat anti-mouse IgG1 followed by addition of *p*-nitrophenyl phosphate substrate. MAb 7B8 binds to the Ag-combining sites of some class II MAbs, such as 12A1 (38).

Peptide ELISA. Microtiter plates were coated with 1 μg of streptavidin/ml and then incubated with 1 μg of biotinylated peptide mimetics/ml and then with parental and variant MAbs. The peptides were PA1 (LQYTPSWMLV), P601.E (SYSWMYE), 206.1 (FGGETFTPDWMMEVAIDNE), and PM14 (CGLQW LWEWPRT), which are described in reference 1. The binding of the MAbs was detected with alkaline phosphatase-conjugated goat anti-mouse IgM, and the plates were developed with *p*-nitrophenyl phosphate (Sigma, St. Louis, Mo.). All incubations were carried out at 37°C for 1 h.

IF. IgM MAbs were added to a suspension of 10^6 *C. neoformans* cells at a concentration of 10 μg/ml in blocking solution (1% BSA, 0.5% horse serum) and incubated at 37°C for 30 min. The cells were then washed twice with blocking solution, incubated with 10 μg of fluorescein isothiocyanate-labeled goat anti-mouse IgM (Southern Biotechnology)/ml for 30 min at 37°C in the dark, washed again with blocking solution, and finally suspended in mounting medium (0.1 M *n*-propyl gallate in PBS) (Sigma). The slides were then viewed with an AX70 microscope (Olympus, Melville, N.Y.) equipped with a standard fluorescein isothiocyanate filter.

Phagocytosis assay. The opsonic efficacies of MAbs 12A1 and 13F1 and the 12A1 mutants were evaluated in J774 macrophage-like cells as described previously (34). A macrophage cell line was used because macrophages are the major phagocytic cells for *C. neoformans* in vivo (14). Briefly, gamma interferon- and lipopolysaccharide-stimulated J774 cells were incubated with *C. neoformans* in the presence and absence of 10 μg of Ab. After incubation for 2 h, the monolayer was washed to remove unbound yeast and the J774 cells were fixed with methanol and stained with Giemsa stain (Sigma). Phagocytosis was determined by counting the numbers of attached and ingested yeast cells using a microscope. Ingested and attached *C. neoformans* cells can be readily distinguished by light microscopy. The phagocytic index was defined as the number of ingested *C. neoformans* cells divided by the number of macrophages.

A. HEAVY CHAIN VARIABLE REGION

	31 CDR1	50 CDR2	80	99 CDR3	IF PATTERN
	S Y F M S W V	T V N S N G D R T Y Y P D T V K G	Y	R D S S G S L Y L A M	
2D10	S Y F M S W V	T V N S N G D R T Y Y P D T V K G	Y	R D S S G S L Y L A M	ANNULAR
12A1	N - - - - - -	M I - I - - N N - - - - - - - - -	D	- - G T F G N - Y - -	ANNULAR
S31N	S - - - - - -	- - - - - - - - - - - - - - - - -	-	- - - - - - - - - - -	ANNULAR
F33Y	- - Y - - - -	- - - - - - - - - - - - - - - - -	-	- - - - - - - - - - -	ANNULAR
M50A	- - - - - - -	A - - - - - - - - - - - - - - - -	-	- - - - - - - - - - -	ANNULAR
I53S	- - - - - - -	- - - S - - - - - - - - - - - - -	-	- - - - - - - - - - -	ANNULAR
N56G	- - - - - - -	- - - - - - G - - - - - - - - - -	-	- - - - - - - - - - -	ANNULAR
N57S	- - - - - - -	- - - - - - - S - - - - - - - - -	-	- - - - - - - - - - -	ANNULAR
D80Y	- - - - - - -	- - - - - - - - - - - - - - - - -	Y	- - - - - - - - - - -	ANNULAR
G103Y	- - - - - - -	- - - - - - - - - - - - - - - - -	-	- - - - Y - - - - - -	ANNULAR
F33Y,N57S	- - Y - - - -	- - - - - - - S - - - - - - - - -	-	- - - - - - - - - - -	PUNCTATE
13F1	- - Y - - - -	A I - - - - G S - - - - - - - - -	Y	- - G T Y - N - Y - -	PUNCTATE
21D2	D - Y - Y - -	Y - S N G - - S - - - - - - - - -	L	- - - - - G Y - - - -	PUNCTATE

B. LIGHT CHAIN VARIABLE REGION

	14	20	24 CDR1	51	54	55 CDR2	94 CDR3	IF PATTERN
	S	S	R S S Q S L V N G N T Y L M	L	Y	F Y S N R F S G	S Q S T H V P W T	
2D10	S	S	R S S Q S L V N G N T Y L M	L	Y	F Y S N R F S G	S Q S T H V P W T	ANNULAR
12A1	G	T	- - - - - - - - - - Y - - - -	V	N	- - - - - - - -	- - - - - - - - -	ANNULAR
13F1	-	-	- - - - - - - - - - - - - - -	-	-	- - - - - - - -	- - - - - - - - -	PUNCTATE
21D2	-	-	- - - - - - - - - - - - - - -	-	-	- - - - - - - -	- - - - - - - - -	PUNCTATE

FIG. 1. V_H and V_L amino acid sequences for MAbs 2D10, 12A1, and 13F1 and the 12A1 V_H mutants. Boxes indicate the amino acid residues shared by the three MAbs which produce a punctate binding pattern.

Measurement of zeta potential. The zeta potential (ζ) is a measurement of cellular charge (in millivolts) that is defined as the potential gradient that develops across the interface between a boundary liquid in contact with a solid and the mobile diffuse layer in the body of the liquid (41). It is derived from the equation $\zeta = 4\pi\eta m/D$, where D is the dielectric constant of the medium, η is the viscosity, and m is the electrophoretic mobility of the particle (41). Cells grown in Sabouraud broth (SAB) were collected and washed three times in 0.01 M NaCl (pH 7.0). The zeta potentials of suspensions of 10^6 cells/ml were measured using a Zeta-Meter (Staunton, Va.) 3.0+ instrument, which determines the zeta potentials of individual suspended cells. The zeta potentials of 10 randomly selected *C. neoformans* cells were measured for each MAb tested. Similar methods have previously been used to measure cellular charge for *C. neoformans* in the presence and absence of Ab (36).

Scanning electron microscopy. *C. neoformans* cells were grown in SAB, the cells were collected and washed three times with PBS, and aliquots of 10^6 cells/ml were incubated with 10 μg of each MAb/ml for 1 h at room temperature. The cells were washed three times in PBS and then incubated in 2.5% glutaraldehyde for 1 h at room temperature. Samples were then applied to a polylysine-coated coverslip and serially dehydrated in alcohol. The samples were fixed in a critical-point drier (Samdri-790; Tousimis, Rockville, Md.), coated with gold-palladium (Desk-1; Denton Vacuum, Inc., Cherry Hill, N.J.), and viewed using a JSM-6400 (JEOL USA, Peabody, Mass.) scanning electron microscope. At least 20 cells were imaged for each MAb tested, and representative photographs were taken. This methodology has previously been used to study the effects of MAbs to *C. neoformans* (12).

Locations of mutations in protein structure. The X-ray structure of the Ab 2H1 in complex with the peptide PA1 is deposited in the Protein Data Bank under accession number 2H1P (47). Mutated amino acid positions in the 12A1 V_H were analyzed on the 2H1 structure using the program RASTOP (42), which is available as free software at http://www.bernstein-plus-sons.com/software/rastop.

Nucleotide sequence accession numbers. The 12A1 and 13F1 V_H sequences are deposited in GenBank under accession numbers AF052834 and AF052835, respectively. The V_L sequences of the two MAbs are deposited in GenBank under accession numbers AF071060 and AF071061, respectively.

RESULTS

Sequences of 12A1 and 13F1. Prior studies had reported partial V_H and V_L sequences of MAbs 12A1 and 13F1 obtained by direct sequencing of mRNA (29). For both MAbs the V_H and V_L sequences were completed, and we also determined the complete constant (C)-region sequence for each IgM. The rationale for determining the C-region sequence was to exclude the unlikely possibility that the serological differences in the binding of these MAbs to GXM were the result of Fc-region differences. For both MAbs, the IgM C regions were identical and corresponded to the IgM(b) sequence (24). The 12A1 and 13F1 V_H sequences differ at eight amino acid positions (Fig. 1). The V_H and V_L amino acid sequences for MAbs 12A1 and 13F1 and other MAbs used in this study are shown in Fig. 1.

Generation and characterization of 12A1→13F1 mutants by site-directed mutagenesis. Expression of the 12A1 V_H in hybridoma 12A1 heavy-chain-loss mutant cells expressing the 12A1 V_L (12A1V_H-12A1V_L) yielded an Ab that produced, as expected, an annular pattern on *C. neoformans* cells, like that of the parent MAb 12A1. Expression of the 12A1 V_H in hybridoma 13F1 heavy-chain-loss mutant cells expressing the 13F1 V_L (12A1V_H-13F1V_L) also resulted in an Ab that produced an annular IF pattern, strongly suggesting that the differences in IF patterns were attributable to differences in V_H sequences. To investigate the contribution of each of the eight amino acid residues that constitute the difference between the V_Hs of MAbs 12A1 and 13F1, we used site-directed mutagenesis to change the 12A1 V_H residues that were different into

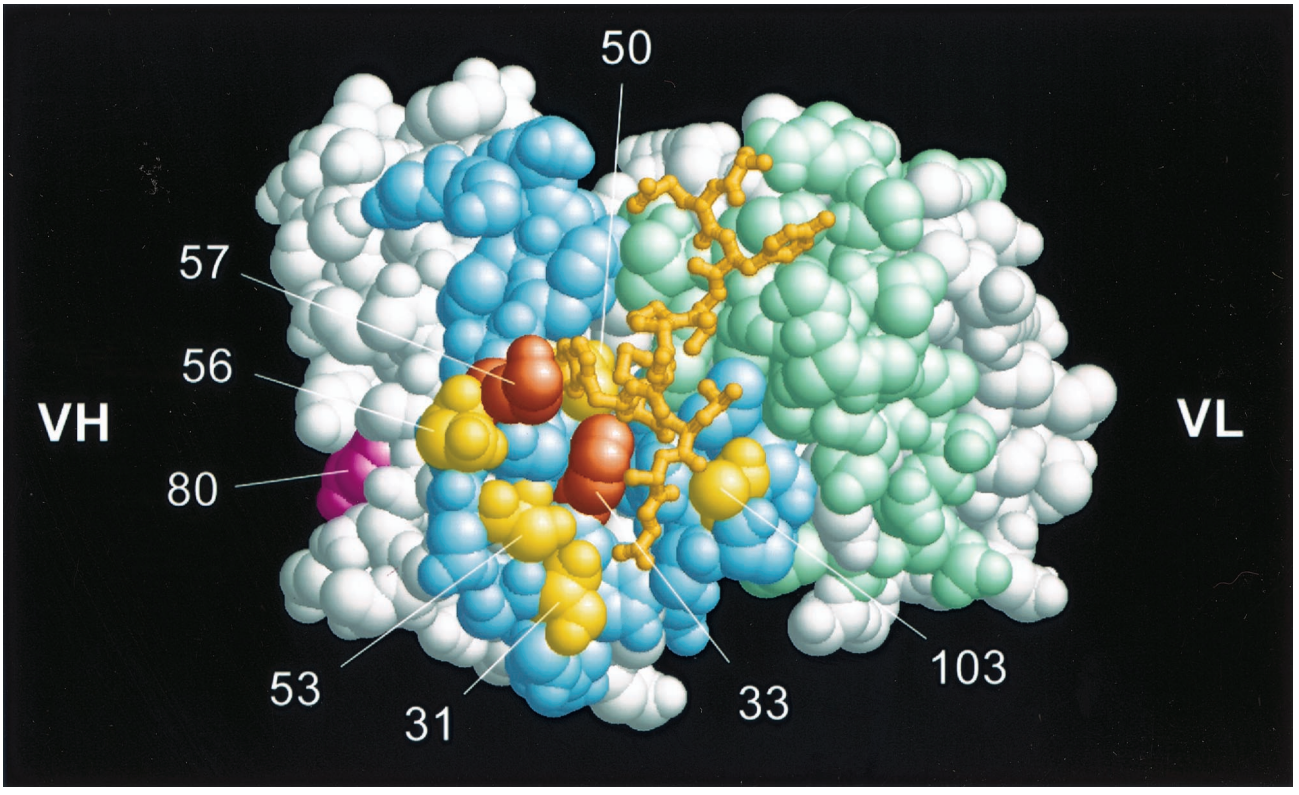

FIG. 2. Three-dimensional representation of the Ag binding site of MAb 12A1 with van der Waals surface. The model is based on the 2H1 structure in complex with the peptide PA1 (47). CDR surfaces are shown colored pale blue (V_H) and light green (V_L). The amino acid positions of MAb 12A1 which were mutagenized are shown in yellow, except for position 80 in magenta, located in the V_H framework, and positions 33 and 57 corresponding to the double mutation. Amino acids at these positions for MAbs 2H1, 12F1, and 13F1, respectively, are as follows: 31, S, N, and S; 33, F, F, and Y; 50, M, M, and A; 53, S, I, and N; 56, D, N, G; 57, K, N, and S; 80, L, D, and Y; and 103, A, F, and Y.

the corresponding 13F1V_H residue (12A1→13F1 mutants). The changes made to the 12A1 V_H are shown in Fig. 1. Figure 2 shows the locations of the induced mutations on a three-dimensional representation of the MAb 12A1 binding site. All 12A1→13F1 mutants bound to GXM as determined by ELISA (Table 1).

All MAb 12A1 V_H variants with single mutations produced an annular IF pattern upon binding strain 24067 (some are shown in Fig. 3). However, there were some differences in the location and intensity of each variant such that none were identical to the IF pattern produced by the parent MAb 12A1 (data not shown). Scanning electron microscopy revealed differences in capsule binding for some of the variants (Fig. 4). Hence, mutational analysis of the 12A1 V_H revealed that al-

TABLE 1. Serological characteristics of MAbs 12A1 and 13F1 and the 12A1→13F1 mutants

Antibody	Reactivity by direct ELISA[a]	Inhibition with MAb 3E5[b]	Reactivity with anti-idiotypic MAb 7B8[c]	Phagocytic index[d]	Immuno-fluorescence
12A1	+++	Yes	+	+++	Annular
13F1	+	No	−	−	Punctate
12A1V_H-12A1V_L	+++	Yes	+	+++	Annular
12A1V_H-13F1V_L	+++	Yes	−	+++	Annular
N31S	+++	Yes	+	+	Annular
F33Y	++	Yes	+	+	Annular
M50A	+++	Yes	+	++	Annular
I53S	+++	Yes	+	++	Annular
N56G	+++	Yes	+	++	Annular
N57S	++	Yes	+	+	Annular
D80Y	+++	Yes	+	++	Annular
F33Y N57S	+	No	−	−	Punctate

[a] Plus signs indicate the relative reactivity of the Ab for GXM as measured by direct ELISA, ranging from weak (+) to strong (+++).
[b] For representative data, see Fig. 5.
[c] +, reactivity; −, lack of reactivity. Data are in Fig. 7.
[d] Plus signs indicate the relative opsonic efficacies of these MAbs; minus signs indicate absence of or minimal opsonic efficacy. For details of phagocytic indices observed with MAbs 12A1 and 13F1, see reference 11.

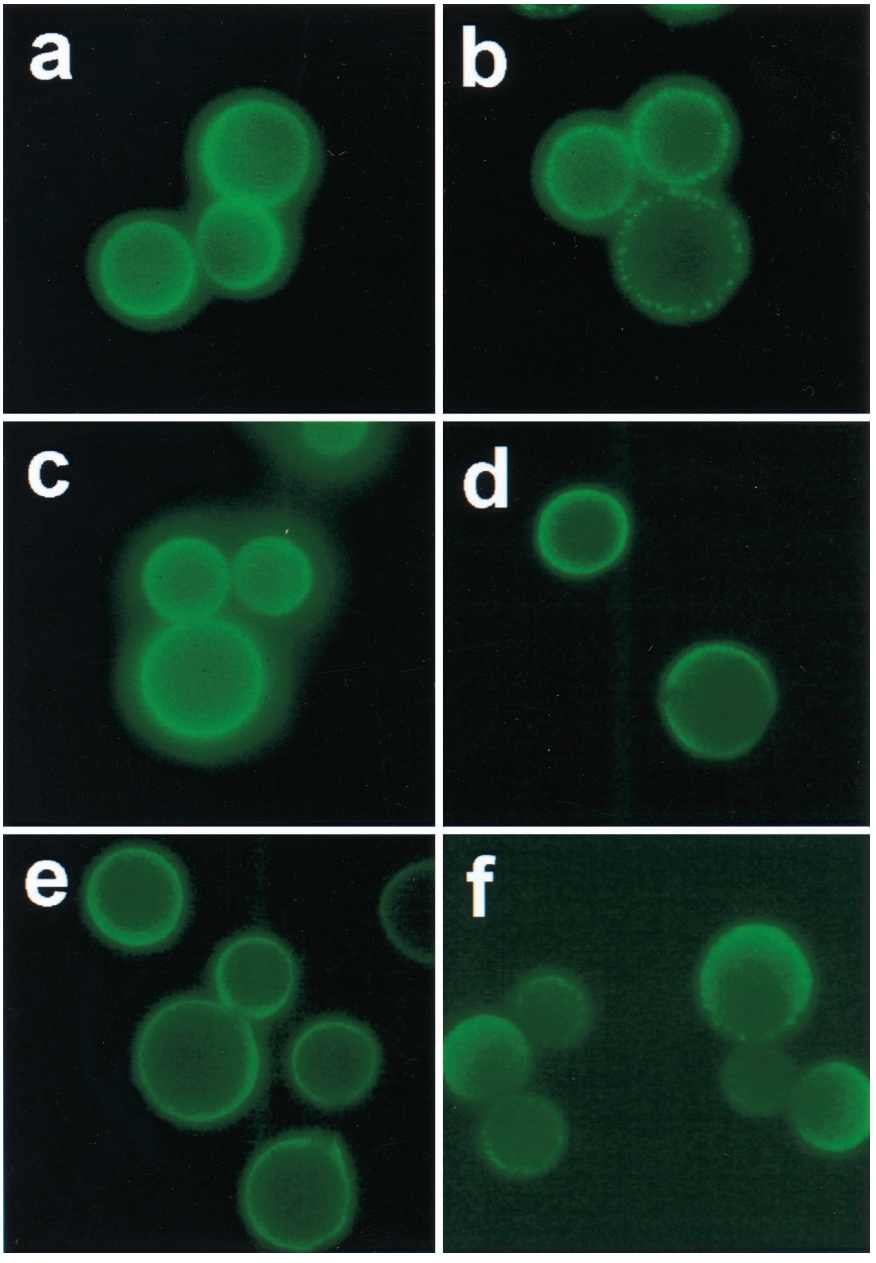

FIG. 3. IF patterns produced by parental MAbs 12A1 (a) and 13F1 (b) and variants 12A1V_H-12A1V_L (c), M50A (d), D80Y (e), and the F33Y N57Y double mutant (f). Magnification, ×250.

though single amino acid changes were not sufficient to alter the IF pattern from annular to punctate, some of the changes produced subtle differences in the binding to the capsule as measured by IF and scanning electron microscopy. Maintenance of the IF pattern in variants with one amino acid change suggested that more than one change would be needed to alter the IF pattern. Faced with the fact that a complete analysis of this system would require an overwhelming effort in the form of constructing the many combinations possible given the amino acid differences between 12A1 and 13F1, we opted for a targeted evaluation.

Another IgM (21D2) had been shown to also produce a punctate IF on strain 24067 and not to be protective (39). MAb 21D2 is a class II MAb that was generated from a mouse with *C. neoformans* infection and recognizes a different epitope than MAb 12A1 on the basis that it can bind to de-O-acetylated GXM. Comparison of the MAb 13F1 and 21D2 sequences revealed that they shared two amino acids at positions 33 and 57 that were not found in the protective IgMs that produced annular IF (Fig. 1). On the basis of this similarity, we constructed a 12A1 V_H with the amino acid changes F33Y and N57S, and this V_H produced a punctate pattern when assembled with the 12A1 V_L (Fig. 3). Thus, introduction of two amino acid changes corresponding to those in MAb 13F1 converted the MAb 12A1 IF from annular to punctate.

As a second measure for specificity we carried out compe-

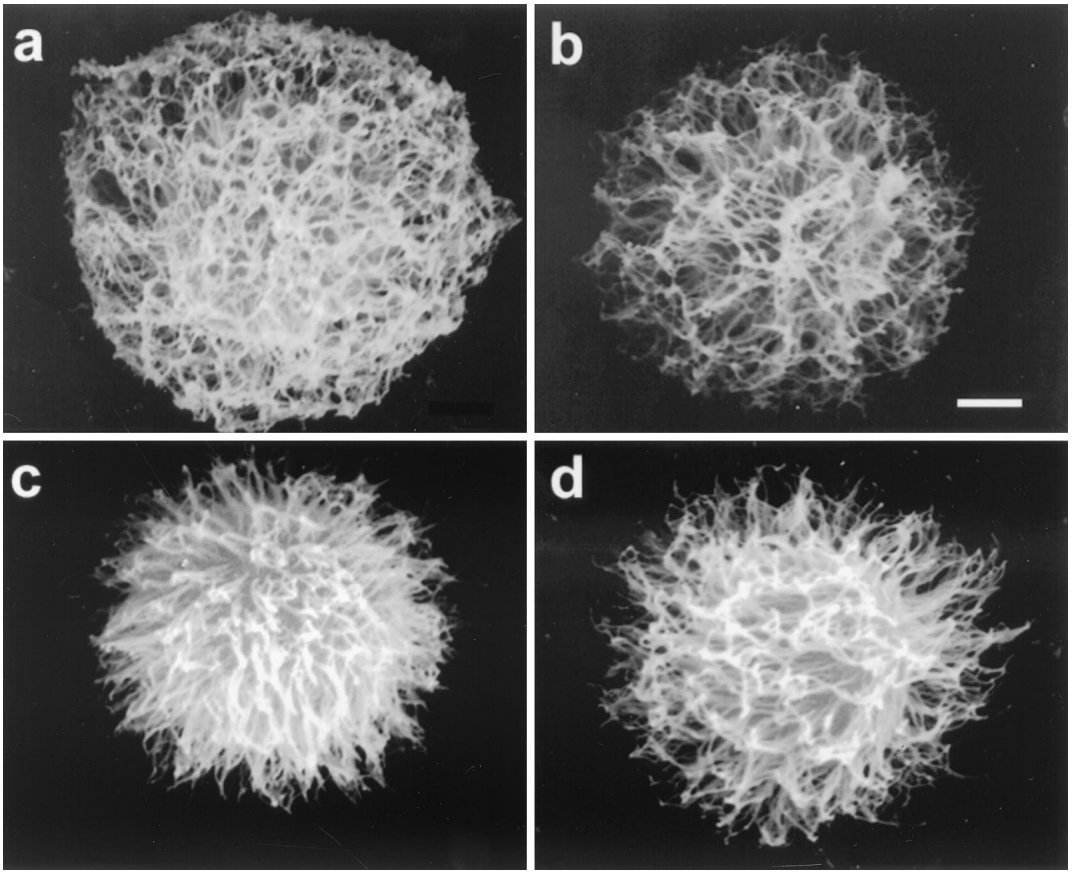

FIG. 4. Scanning electron micrographs of yeast cells coated with MAbs 12A1V_H-12A1V_L (a), 13F1 (b), F33Y (c), and the F33Y N57Y double mutant (d). Bar, 10 μm. For each Ab at least 15 to 20 cells were imaged, and representative yeast cells are shown.

tition assays with MAb 3E5, which competes with MAb 12A1 but not 13F1 for GXM binding by ELISA (31). Like the parent MAb 12A1, all 12A1→13F1 mutants displaying single amino acid changes were inhibited by MAb 3E5 (Table 1). However the mutant having two amino acid changes at F33Y and N57S was not inhibited by MAb 3E5 (Fig. 5). MAb 21D2 was also not inhibited by MAb 3E5 (data not shown). Hence, introduction of two amino acids changed the specificity of MAb 12A1 to one that is indistinguishable from that of MAb 13F1 by this assay.

Reactivities of MAbs 12A1 and 13F1 and 12A1→13F1 mutants with peptide mimotopes of MAb 2H1. The crystal structures of MAb 2H1 with and without a peptide mimotope in the binding site are available (47). Since MAbs 12A1 and 13F1 use V-region genes of the same family, share the 2H1 idiotype, and have very similar serological characteristics (5), we analyzed their reactivities with peptide mimotopes of GXM recognized by MAb 2H1 (Table 2). Neither MAb 12A1 nor MAb 13F1 showed significant reactivity with peptide PA1, 601, or 206.1, which are mimotopes of GXM that bind strongly to MAb 2H1 and the other class II Abs, such as MAb 2D10. Interestingly, the 12A1V_H-13F1V_L hybrid reacted with peptide 206.1 despite no reactivity by their parent MAbs. The 12A1→13F1 mutants I53S, N56G, and N57S each reacted strongly with peptide 206.1. Hence, the introduction of single mutations into the 5′ region of the 12A1 V_H CDR altered the specific ability of MAb 12A1 to recognize a GXM peptide mimetic even when no change in IF pattern after binding *C. neoformans* was apparent.

Phagocytosis assays. MAb 12A1 is significantly more opsonic than MAb 13F1 for *C. neoformans* cells (11). The 12A1→13F1 mutants each were less opsonic than the parent MAb 12A1, and mutations F33Y and N57S significantly reduced the opsonic potential of the Ab (Table 2). The double mutation at F33Y and N57S resulted in complete loss of opsonic activity to a level comparable to that observed for MAb 13F1 (Table 2). Hence, the F33Y N57S double mutant is like MAb 13F1 with respect to opsonization efficacy.

Zeta potential. *C. neoformans* cells have a very high negative charge relative to other yeast cells, which has been attributed to the polysaccharide capsule (36, 37). Ab binding to the *C. neoformans* capsule can result in changes to the yeast cell charge (36). This phenomenon is not well understood, but our mutant set provided the opportunity to investigate whether amino acid changes could alter the zeta potential of *C. neoformans* cells independent of their effects on Ab charge. Measurements of zeta potential of *C. neoformans* cells after binding MAb 12A1 or 13F1 or the 12A1→13F1 mutants revealed relatively small changes to the yeast cell charge after Ab binding, even for the D80Y mutant, which involved replacement of a negatively charged aspartic acid with a neutral tyrosine (Fig. 6). The largest change was observed for N56G, which conferred a significantly greater negative charge to *C. neoformans* than

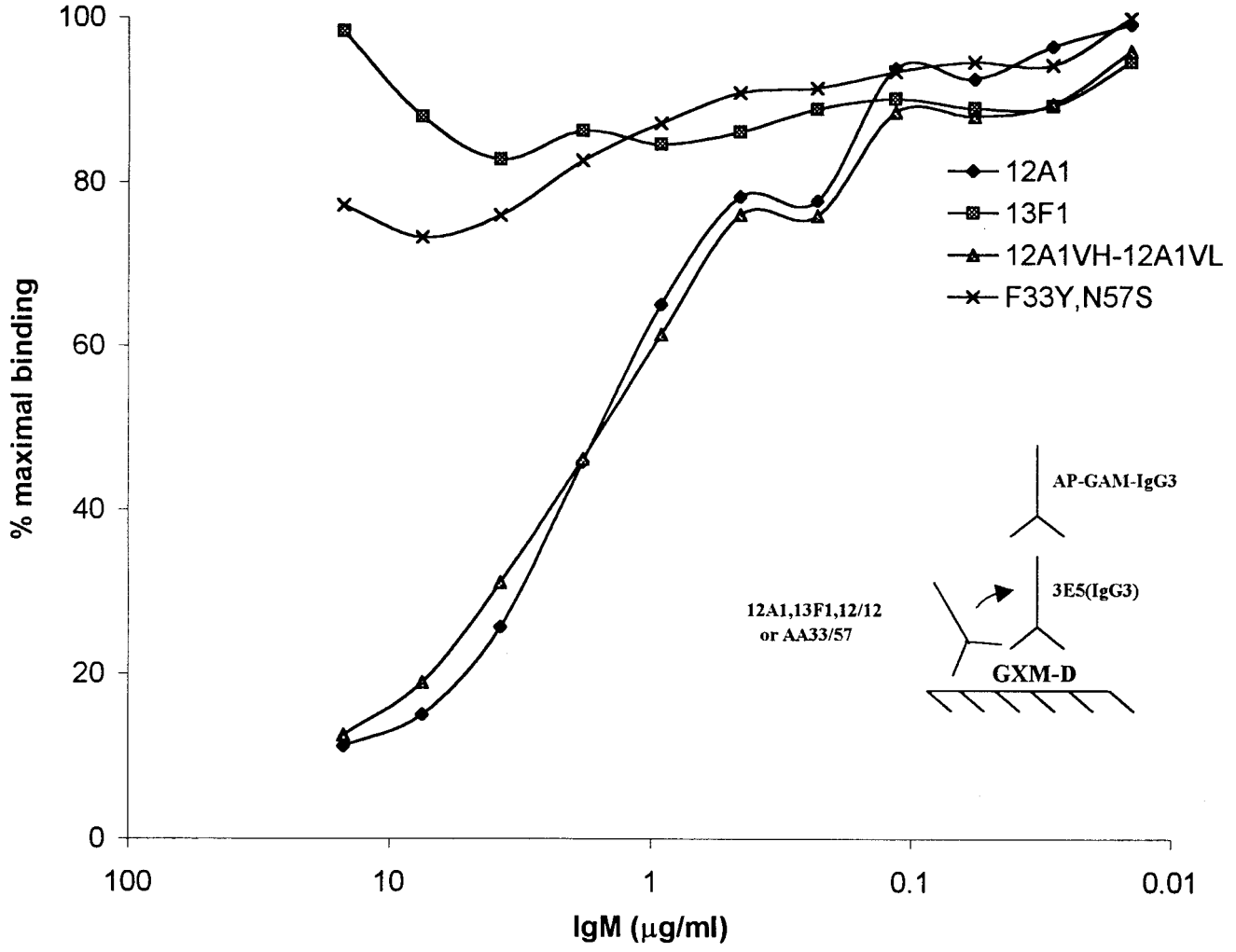

FIG. 5. Competition ELISA between Abs 12A1, 13F1, 12A1V_H-12A1V_L, and the F33Y N57Y double mutant with the IgG3 MAb 3E5. At increasing concentrations of MAbs 12A1 and 12A1V_H-12A1V_L the binding of MAb 3E5 is inhibited. In contrast, no significant inhibition of MAb 3E5 binding is produced by either MAb 13F1 or the F33Y N57Y double mutant. AP-GAM-IgG3, alkaline phosphatase-conjugated anti-mouse IgG3.

MAb 12A1 despite involving a replacement of a neutral asparagine with a neutral glycine (Fig. 7).

Reactivity with anti-idiotypic Ab. MAb 7B8 binds to the Ag-combining sites of some class II MAbs (38). MAb 7B8 binds to Abs 12A1, 12A1V_H-12A1V_L, and 2D10 but not to 13F1 or the 12A1V_H-13F1V_L hybrid (Fig. 7). MAb 7B8 reacted with all 12A1→13F1 mutants except the F33Y N57S double mutant. These results indicate that the idiotypic determinants recognized by MAb 7B8 reside in both the V_H and V_L and at V_H positions 33 and 57.

Frequency of Y33 and S57 in the V_Hs of Abs to GXM and germ line 7183 genes. None of the 14 MAbs to GXM that use V_H7183 gene family segments and are protective in mice have Y33 or S57 (Table 3). Two of 15 V_H7183 family gene segments in the genetic database have Y33, six have S57, and only two (V_H50.1 and V_H7183.10) have both Y33 and S57.

TABLE 2. Reactivities of several MAbs and 12A1→13F1 variants with peptide mimotopes of GXM

Antibody	Reactivity[a] with peptide:			
	PA1	601	206.1	PM14
2D10	+	+++	+++	+
2H1	+++	++	+++	+
21D2	−	−	+++	−
12A1	−	−	+	−
13F1	−	−	−	+++
12A1V_H-13F1V_L	−	−	+	−
12A1V_H-13F1V_L	−	−	+	−
N31S	−	−	−	−
F33Y	−	−	−	++
M50A	−	−	−	−
I53S	−	−	++	−
N56G	−	−	+++	−
N57S	−	−	−	−
D80Y	−	−	+++	−
F103Y	−	−	−	−
F33Y N57S	−	−	−	−

[a] Plus and minus signs indicate the relative reactivities of the various Abs for the peptide as measured by ELISA, ranging from none (−) to weak (+) to strong (+++).

DISCUSSION

Characterization of the amino acids residues responsible for Ab specificity to *C. neoformans* polysaccharide is important for

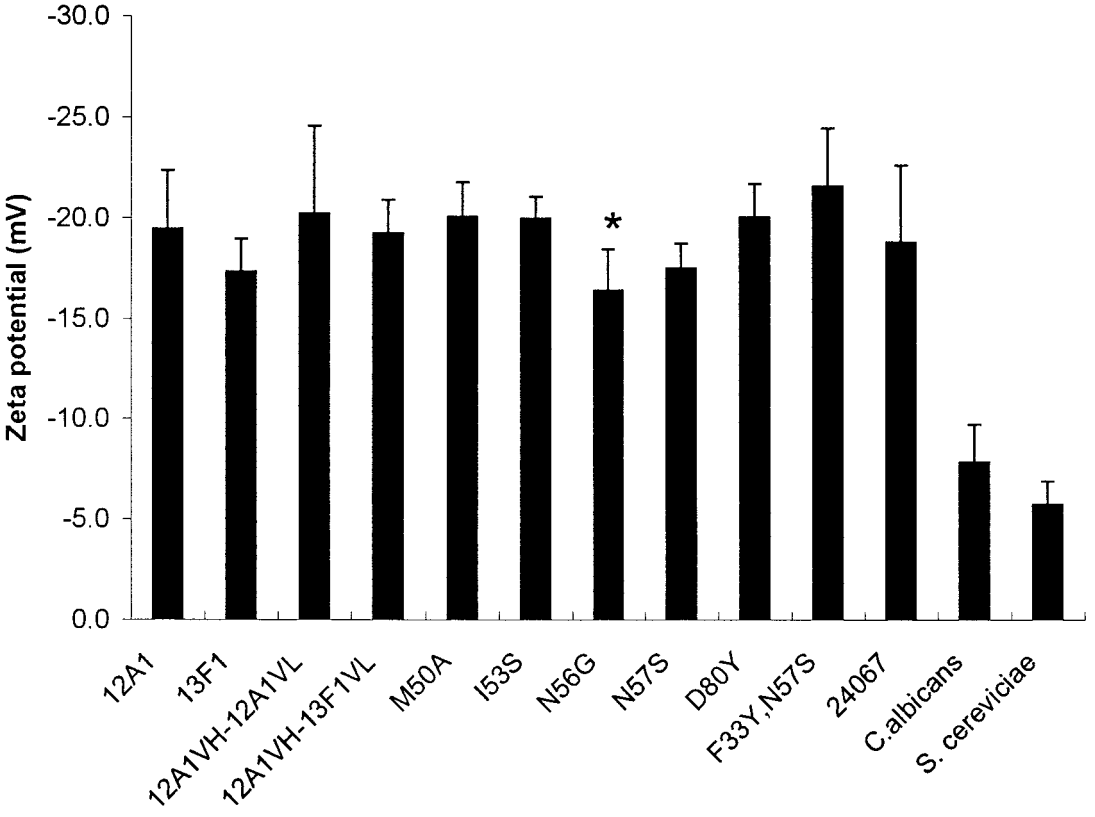

FIG. 6. Zeta potentials of *C. neoformans* cells coated with MAbs 12A1 and 13F1 and the various 12A1→13F1 mutants. *, the zeta potential of the N56G variant was significantly lower ($P = 0.017$) than that of the parent MAb 12A1. Error bars indicate standard deviations.

understanding the relationship between Ab structure and protective efficacy. This information can also be helpful for preserving fine specificity of Abs to *C. neoformans* during Ab engineering and for the ongoing efforts to develop vaccines using polysaccharide-protein conjugates (6, 13) and peptide mimotopes (1).

Our results show that changing two amino acids in the binding pocket of the protective IgM MAb 12A1 V_H to the corresponding residues in the V_H of the nonprotective MAb 13F1 can alter the IF pattern and significantly reduce the opsonic activity, such that the mutated 12A1 Ab behaves like MAb 13F1. We were able to target these amino acids because we had available V_H and V_L sequences of four closely related class II IgM MAbs (8, 29), namely, 12A1, 13F1, 2D10, and 21D2, that differed in IF pattern despite having very similar V-region sequences. We focused our efforts on analyzing V_H rather than V_L differences as the cause of differences in IF patterns because the MAb 2D10 and 13F1 V_Ls were identical yet produced annular and punctate IF patterns, respectively. This deduction was confirmed by the findings that the 12A1V_H-13F1V_L hybrid produced annular IF and that mutations to the 12A1 V_H amino acids changed the IF pattern from annular to punctate. The observation that the 12A1 V_H is responsible for the type of pattern observed is consistent with the proposal that Ab specificity is frequently determined by the V_H (23).

Superposition of the V-region sequence of MAb 12A1 on the crystal structure of the closely related MAb 2H1 revealed that all of the mutated amino acid positions with the exception of framework position 80 mapped to the Ag binding site. Nonetheless, the data showed that single amino acid changes in the sequence of MAb 12A1 to the comparable residues in MAb 13F1 were insufficient to change the IF pattern or to affect the outcome of competition experiments with MAb 3E5. However, when the two amino acids in the 12A1 V_H at positions 33 and 57 were changed to the amino acids found in the 13F1 V_H, a punctate pattern was observed. Competition experiments confirmed that the two mutations conferred a specificity change, since the parent but not the F33Y N57S double mutant competed for GXM with MAb 3E5.

The punctate and annular IF patterns are considered to be a consequence of the binding of MAbs 12A1 and 13F1 to different epitopes, because these MAbs have similar affinities for GXM although they (i) bind to different places in the capsule of serotype D strains (15), (ii) bind differently to serotype A and D strains (11), (iii) exhibit differences in binding to peptide mimetics (43), (iv) react differently with polysaccharides from the four *C. neoformans* serotypes (6), and (v) demonstrate differences in competition experiments (31). Given that the annular and punctate binding patterns correlate with protective and nonprotective efficacy, respectively, and reflect the binding of Abs with different specificities, the V_H positions 33 and 57 define critically important structural correlates for Ab functional efficacy against *C. neoformans*.

The Ab response to GXM is highly restricted in V gene usage, even among genetically different strains of mice (5, 8, 29, 38, 40, 49). The overwhelming majority of murine MAbs

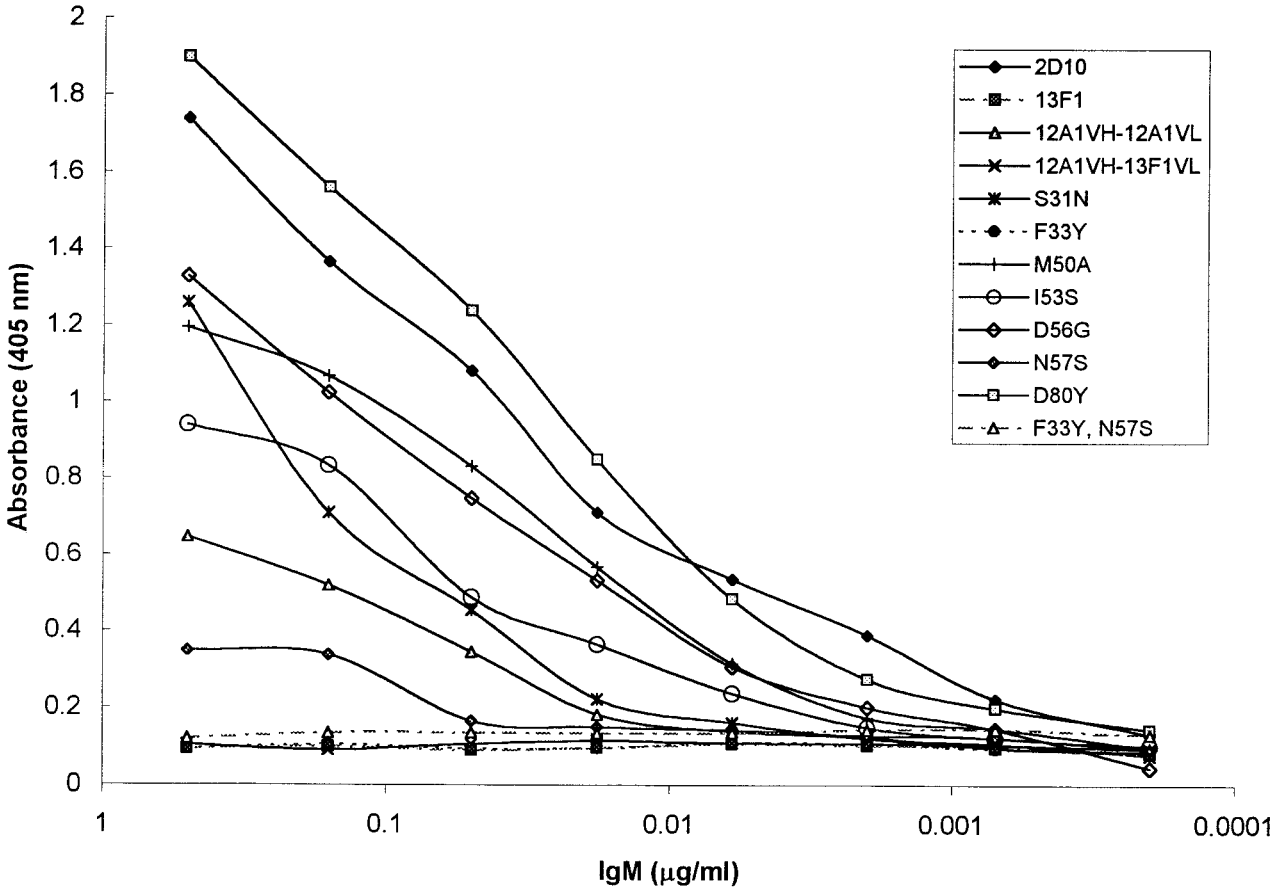

FIG. 7. Reactivities of MAbs 12A1 and 13F1 and various 12A1→13F1 mutants with the anti-idiotypic MAb 7B8 as determined by ELISA.

use 7183 V_H gene family elements (5, 38). The F33 and N57 in MAb 12A1 are both found in the consensus V_H sequence from which the 12A1 V_H was derived (29). Since only two 7183 V_H family genes have both Y33 and S57 in their germ line sequences, this implies that F33 and N57 are likely to have arisen from somatic mutations that accrued during the immune response. Alternatively, they are derived from a germ line V_H7183 family gene element that has not yet been characterized. Regardless of their origin, the Y33 and S57 residues in MAb 13F1 appear to have changed the specificity from a GXM epitope that could mediate protection against serotype D strains to one that could not. None of the 12 protective MAbs for which sequence data are available has the Y33 and S57 motif. In contrast, the two nonprotective class II MAbs for serotype D strains each have Y33 and S57. Analysis of germ line 7183 gene family sequences in the genetic database (GenBank, Los Alamos, N.Mex.) indicates that 13% have F33, 40% have N57, and 15% have both F33 and N57. One of two gene elements with the Y33 and S57 motif is V_H50.1, and it is used in the nonprotective MAb 21D2 in its germ line configuration (8). These results suggest that nonprotective Abs can be generated either from germ line sequences or as a consequence of somatic mutation. For many 7183 V_H gene elements, a single somatic mutation can yield the F33 and N57 motif found in MAb 13F1. The ability of the mouse genome to code for both protective and nonprotective specificities may underlie such perplexing observations as the fact that highly immunogenic polysaccharide-protein conjugate vaccines can elicit high-titer protective (13) and nonprotective (18) Ab responses. The implication that germ line residues in CDRs are critical for the

TABLE 3. Amino acid usage at positions 33 and 57 for antibodies of *C. neoformans* which have been evaluated for protective efficacy

MAb	Isotype	Amino acid at position:		Protective	Reference(s)
		33	57		
Consensus	NA[a]	F	N	NA	29
3B10	IgG1	F	N	Yes	29, 33
2D10	IgM	F	R	Yes	29, 32
2H1	IgG1	F	K	Yes	29, 32
3E5	IgG1[b]	F	N	Yes	8, 29, 48
18G9	IgA	F	K	Yes	29, 32
10F10	IgG1	F	S	Yes	29
12A1	IgM	F	N	Yes	29, 31
17E12	IgG1	F	K	Yes	29
18B7	IgG1	F	K	Yes	29
3C2	IgG1	L	K	Yes	5, 30
471	IgG1	L	K	Yes	5, 30
13F1	IgM	Y	S	No	29, 31
21D2	IgM	Y	S	No	8, 32

[a] NA, not applicable.
[b] The IgG1 switch variant of the nonprotective IgG3 MAb 3E5 is protective (48).

annular IF pattern that is associated with Ab efficacy is consistent with the proposal that certain V_H genes are required for carbohydrate binding (45) and the fact that class II Abs to GXM are all derived from the same Ab clan (25).

Our observations demonstrate that a change of IF pattern from annular to punctate required changes in at least two amino acids located in each of the CDR1 and CDR2 V_H regions. However, scanning electron microscopy revealed differences in the fibrillar structure after binding of MAbs 12A1 and 13F1 and the $12A1V_H \rightarrow 13F1V_H$ mutants. Previous work has shown that fibrillar capsular structure is different after binding of MAbs 12A1 and 13F1 (12). Thus, each mutant with a single amino acid change displayed qualitative alterations in the annular IF pattern after binding to strain 24067. Although caution is always warranted when interpreting or comparing scanning electron micrographs of polysaccharide capsules (12), the differences in fibrillar appearance are consistent with the notion that some amino acid replacements affected the interaction with the capsule even though the annular IF pattern was maintained. This raises the possibility that Ab reactivity with *C. neoformans* in the punctate pattern reflects a continuum based on deviations from the consensus and/or germ line motif found in 12A1, although more work is needed to determine precisely how certain Abs react with GXM.

The F33Y change occurs at one of five amino acid residues delineating a cavity at the bottom of the MAb 2H1 structure. The side chains of F33 or Y33 at this position are near the surface of this cavity in a location that is likely to be solvated and in contact with the polysaccharide. Hence, it appears that F33 is in a strategic position to affect the type of binding that occurs but that a single change at this location is not sufficient to alter the IF pattern. Instead, the second change of N57S is also required, and the double mutation significantly reduced the binding to GXM determined by ELISA in a manner comparable to that for MAb 13F1. These results imply that amino acid residues in V_H define the epitope specificity for these Abs to *C. neoformans,* although both V_H and V_L contribute to Ag affinity. A similar observation has been reported for Abs to digoxin (35), whereas for Abs to the polysaccharide levan, residues affecting fine specificity were located in the V_H-V_L junctional area (2).

Greenspan has defined an Ab paratope involved in a given Ag-Ab interaction as contact-, affinity-, and specificity-determining residues which may confer overlapping but nonidentical interactions with the epitope (19) and has defined amino acids that contribute to binding as the paratope set, depending on whether the residue is involved in contact, bond formation, or both (19). Our results are consistent with this view and suggest that each amino acid change to the paratope resulted in an alteration in the type of Ag-Ab complex formed in the capsule. Hence, the annular and punctate patterns may simply represent two forms of Ab binding to GXM among a multitude of possible interactions defined by the paratope of class II MAbs to GXM.

Ab binding in annular IF patterns is associated with significantly greater opsonic efficacy (10, 39). The 12A1→13F1 variants each resulted in reduced opsonic efficacy relative to that of the parent MAb 12A1, but the greatest effects for single amino acid changes were observed with F33Y and N57S. Both the F33Y and N57Y mutations significantly reduced the opsonic efficacy of the Ab without altering the IF pattern from annular to punctate. However, when both mutations were present simultaneously, the opsonic efficacy was further reduced to that of MAb 13F1. Hence, the change in IF pattern from annular to punctate which resulted from this double mutation also abolished the opsonic efficacy of this MAb 12A1→13F1 mutant. The finding that the change from annular to punctate reactivity was accompanied by a reduction in Ab opsonic efficacy establishes an association between Ab structure and biological function. This defines a key structure-function relationship for Abs to *C. neoformans* that is relevant to the choice of immunotherapeutic reagents and vaccine design.

IgG1 binding to the *C. neoformans* capsule alters the charge of the cell, but the mechanism for this phenomenon is not understood (36, 37). However, neither IgM MAb 12A1 nor 13F1 produced significant changes in cell charge upon binding *C. neoformans*. Since our mutant Ab set included mutations that replaced charged and neutral residues, we investigated the effect of amino acid replacements on the zeta potential of IgM-coated cells in an attempt to gain insight into this phenomenon. The various amino acid substitutions had little effect on the cell charge of *C. neoformans* after Ab binding. Replacement of a negatively charged aspartic acid at position 80 with a neutral tyrosine had no significant effect on the zeta potential of IgM-coated cells. Interestingly, the largest change in zeta potential was observed with N56G replacement, which involved the substitution of a neutral amino acid residue for another. This result suggests that cell charge can change upon Ab binding without an apparent change in the Ab charge.

The anti-idiotypic MAb 7B8 binds to the MAbs 12A1 and $12A1V_H$-$12A1V_L$ but not to MAb 13F1. No binding to the $12A1V_H$-$13F1V_L$ hybrid was observed, indicating that amino acid differences between the 12A1 V_L and 13F1 V_L contribute to defining the idiotype. In contrast, MAb 7B8 recognized all of the 12A1→13F1 single-amino-acid-mutated variants, and several exhibited significantly stronger binding than the parent MAb 12A1, suggesting that those changes stabilized the Ab-Ab interaction. However, there was no reactivity with the F33Y N57Y double mutant, indicating that F33 and N57 are part of the idiotype recognized by MAb 12A1. Hence, the same residues that confer annular or punctate specificity in the V_H chain are involved in recognition by the 7B8 anti-idiotypic Ab. These studies suggest that this reagent may be useful for identifying protective MAbs.

Peptide mimetics of class II MAbs have been shown to bind in the Ab combining site and to be useful in mapping the epitope specificities of closely related MAbs (43, 44, 47). Peptide mimetics for MAb 12A1 and 13F1 have been reported (39). The availability of multiple MAb 12A1 mutants expressing the corresponding MAb 13F1 amino acid provided the opportunity to ascertain whether the same residues were responsible for peptide and binding pattern specificities. To our knowledge this is the first study that has simultaneously evaluated the contributions of V-region residues to the binding of polysaccharide Ag and a peptide mimotope. PA1 is a 10-mer peptide that binds to the closely related MAbs 2H1 and 2D10 but not to MAbs 12A1, 13F1, and 21D2 or to any of the variants generated here. The crystal structure has shown that PA1 has significantly more van der Waals interactions with V_L than with V_H. Hence, even though MAbs 2D10, 13F1, and

21D2 have the same V_L, their interactions with PA1 are not sufficient to promote binding in the absence of specific V_H interactions. Similar results were obtained with the 6-mer peptide 601, which includes the same motif as peptide PA1 which is involved in Ab combining site binding. In contrast, 206.1 is a 19-mer peptide that binds MAbs 2D10, 2H1, and 21D2 strongly, 12A1 weakly, and 13F1 not at all. The larger size of 206.1 is believed to make it capable of making additional contacts with the Ab binding region. The I53S, N56G, and D80Y mutants exhibited stronger binding to peptide 206.1 than either MAb 12A1 or 13F1. The results with peptide 206.1 indicate a dissociation of the binding characteristics of Ab with polysaccharide and peptide, suggesting that different residues are responsible for binding the GXM Ag and the peptide mimetic. This is consistent with the suggestion that peptide mimotopes of carbohydrate-binding Abs are recognized by different mechanisms than the carbohydrate Ag (21). However, in the case of peptide PM14, which reacts with MAb 13F1 but not 12A1, the 12A1 V_H mutant F33Y demonstrated significant reactivity. Since the F33Y N57Y double mutant indicates that the F33Y residue is also involved in the IF binding pattern, it appears that some amino acids in the paratope set bind primarily peptide or carbohydrate, whereas others interact with both types of Ag.

In summary, our results indicate that V_H amino acid residues F33 and N57 are critical determinants for Ab binding to GXM in a manner that translates into Ab-mediated protection against *C. neoformans*. Changing these two amino acids to the corresponding residues in MAb 13F1 resulted in a mutated variant of MAb 12A1 which behaved like MAb 13F1 with regard to IF, phagocytosis, recognition by anti-idiotypic MAb, and binding to GXM. These results are internally consistent and define two molecular determinants for protective efficacy against *C. neoformans*. The difference in reactivity of mutated Abs with GXM and peptide mimetics strongly suggests that different paratopes interacted with the polysaccharide Ag and the peptide mimetic. Hence, the search for peptide mimotopes that can elicit antipolysaccharide responses may be more fruitful if it focuses on peptides that interact with Ab amino acids important for binding carbohydrate epitopes. The implication that the punctate IF specificity can be either encoded in germ line V genes or generated by somatic mutation highlights the complexity and difficulty in consistently eliciting protective Ab responses to *C. neoformans*.

ACKNOWLEDGMENTS

We thank H. Bernstein and R. Sayle for help with the RASTOP program. We are grateful to Liise-anne Pirofski for critical reading of the manuscript.

This work was supported by NIH awards AI33774, AI3342, and HL-59842-01 to A.C. and AI01489 to J.N. A.C. is the recipient of a Burroughs Wellcome Development Therapeutics Award.

REFERENCES

1. **Beenhouwer, D. O., P. Valadon, R. May, and M. D. Scharff.** 2000. Peptide mimicry of the polysaccharide capsule of *Cryptococcus neoformans*, p. 143–160. *In* M. W. Cunningham and R. S. Fujinami (ed.), Molecular mimicry, microbes, and autoimmunity. ASM Press, Washington, D.C.
2. **Brorson, K., C. Thompson, G. Wei, M. Krasnokutsky, and K. E. Stein.** 1999. Mutational analysis of avidity and fine specificity of anti-levan antibodies. J. Immunol. **163:**6694–6701.
3. **Casadevall, A.** 1995. Antibody immunity and invasive fungal infections. Infect. Immun. **63:**4211–4218.
4. **Casadevall, A., W. Cleare, M. Feldmesser, A. Glatman-Freedman, D. L. Goldman, T. R. Kozel, N. Lendvai, J. Mukherjee, L. Pirofski, J. Rivera, A. L. Rosas, M. D. Scharff, P. Valadon, K. Westin, and Z. Zhong.** 1998. Characterization of a murine monoclonal antibody to *Cryptococcus neoformans* polysaccharide that is a candidate for human therapeutic studies. Antimicrob. Agents Chemother. **42:**1437–1446.
5. **Casadevall, A., M. DeShaw, M. Fan, F. Dromer, T. R. Kozel, and L. Pirofski.** 1994. Molecular and idiotypic analysis of antibodies to *Cryptococcus neoformans* glucuronoxylomannan. Infect. Immun. **62:**3864–3872.
6. **Casadevall, A., J. Mukherjee, S. J. N. Devi, R. Schneerson, J. B. Robbins, and M. D. Scharff.** 1992. Antibodies elicited by a *Cryptococcus neoformans* glucuronoxylomannan-tetanus toxoid conjugate vaccine have the same specificity as those elicited in infection. J. Infect. Dis. **65:**1086–1093.
7. **Casadevall, A., J. Mukherjee, and M. D. Scharff.** 1992. Monoclonal antibody ELISAs for cryptococcal polysaccharide. J. Immunol. Methods **154:**27–35.
8. **Casadevall, A., and M. D. Scharff.** 1991. The mouse antibody response to infection with *Cryptococcus neoformans*: V_H and V_L usage in polysaccharide binding antibodies. J. Exp. Med. **174:**151–160.
9. **Cherniak, R., E. Reiss, and S. Turner.** 1982. A galactoxylomannan antigen of *Cryptococcus neoformans* serotype A. Carbohydr. Res. **103:**239–250.
10. **Cleare, W., M. E. Brandt, and A. Casadevall.** 1999. Monoclonal antibody 13F1 produces annular immunofluorescent patterns on *Cryptococcus neoformans* serotype AD isolates. J. Clin. Microbiol. **37:**3080.
11. **Cleare, W., and A. Casadevall.** 1998. The different binding patterns of two IgM monoclonal antibodies to *Cryptococcus neoformans* serotype A and D strains correlates with serotype classification and differences in functional assays. Clin. Diagn. Lab. Immunol. **5:**125–129.
12. **Cleare, W., and A. Casadevall.** 1999. Scanning electron microscopy of encapsulated and nonencapsulated *Cryptococcus neoformans* and the effect of glucose on capsular polysaccharide release. Med. Mycol. **37:**235–243.
13. **Devi, S. J. N.** 1996. Preclinical efficacy of a glucuronoxylomannan-tetanus toxoid conjugate vaccine of *Cryptococcus neoformans* in a murine model. Vaccine **14:**841–842.
14. **Feldmesser, M., Y. Kress, P. Novikoff, and A. Casadevall.** 2000. *Cryptococcus neoformans* is a facultative intracellular pathogen in murine pulmonary infection. Infect. Immun. **68:**4225–4237.
15. **Feldmesser, M., J. Rivera, Y. Kress, T. R. Kozel, and A. Casadevall.** 2000. Antibody interactions with the capsule of *Cryptococcus neoformans*. Infect. Immun. **68:**3642–3650.
16. **Fleuridor, R., R. H. Lyles, and L. Pirofski.** 1999. Quantitative and qualitative differences in the serum antibody profiles of human immunodeficiency virus-infected persons with and without *Cryptococcus neoformans* meningitis. J. Infect. Dis. **180:**1526–1535.
17. **Fleuridor, R., Z. Zhong, and L. Pirofski.** 1998. A human IgM monoclonal antibody prolongs survival of mice with lethal cryptococcosis. J. Infect. Dis. **178:**1213–1216.
18. **Goren, M. B.** 1967. Experimental murine cryptococcosis: effect of hyperimmunization to capsular polysaccharide. J. Immunol. **98:**914–922.
19. **Greenspan, N. S.** 1997. Conceptions of epitopes and paratopes and the ontological dynamics of immunological recognition, p. 383–403. *In* D. H. Rouvray (ed.), Concepts in chemistry: a contemporary challenge. Research Studies Press Ltd., Taunton, Somerset, England.
20. **Han, Y., and J. E. Cutler.** 1995. Antibody response that protects against disseminated candidiasis. Infect. Immun. **63:**2714–2719.
21. **Harris, S. L., L. Craig, J. S. Mehroke, M. Rashed, M. B. Zwick, K. Kenar, E. J. Toone, N. Greenspan, F. I. Auzanneau, J. R. Marino-Albernas, B. M. Pinto, and J. K. Scott.** 1997. Exploring the basis of peptide-carbohydrate crossreactivity: evidence for discrimination by peptides between closely related anti-carbohydrate antibodies. Proc. Natl. Acad. Sci. USA **94:**2454–2459.
22. **Houpt, D. C., G. S. T. Pfrommer, B. J. Young, T. A. Larson, and T. R. Kozel.** 1994. Occurrences, immunoglobulin classes, and biological activities of antibodies in normal human serum that are reactive with *Cryptococcus neoformans* glucuronoxylomannan. Infect. Immun. **62:**2857–2864.
23. **Kabat, E. A., and T. T. Wu.** 1991. Identical V region amino acid sequences and segments of sequences in antibodies of different specificities. Relative contributions of VH and VL genes, minigenes, and complementarity-determining regions to binding of antibody-combining sites. J. Immunol. **147:**1709–1719.
24. **Kabat, E. A., T. T. Wu, H. M. Perry, K. S. Gottesman, and C. Foeller.** 1991. Proteins of immunological interest. Publication no. 91-3242. National Institutes of Health, Bethesda, Md.
25. **Kirkham, P. M., F. Mortari, J. A. Newton, and H. W. Schroeder.** 1991. Immunoglobulin VH clan and family identity predicts variable domain structure and may influence antigen binding. EMBO J. **11:**603–609.
26. **Lendvai, N., and A. Casadevall.** 1999. Antibody mediated toxicity in *Cryptococcus neoformans* infection: mechanism and relationship to antibody isotype. J. Infect. Dis. **180:**791–801.
27. **MacGill, T. C., R. S. MacGill, A. Casadevall, and T. R. Kozel.** 2000. Biological correlates of capsular (quellung) reactions of *Cryptococcus neoformans*. J. Immunol. **164:**4835–4842.
28. **McLean, G., A. Nakouzi, A. Casadevall, and N. S. Green.** 2001. Human and

murine expression vector cassettes. Mol. Immunol. **37:**837–845.
29. **Mukherjee, J., A. Casadevall, and M. D. Scharff.** 1993. Molecular characterization of the antibody responses to *Cryptococcus neoformans* infection and glucuronoxylomannan-tetanus toxoid conjugate immunization. J. Exp. Med. **177:**1105–1106.
30. **Mukherjee, J., T. R. Kozel, and A. Casadevall.** 1998. Monoclonal antibodies reveal additional epitopes of serotype D *Cryptococcus neoformans* capsular glucuronoxylomannan that elicit protective antibodies. J. Immunol. **161:** 3557–3568.
31. **Mukherjee, J., G. Nussbaum, M. D. Scharff, and A. Casadevall.** 1995. Protective and nonprotective monoclonal antibodies to *Cryptococcus neoformans* originating from one B-cell. J. Exp. Med. **181:**405–409.
32. **Mukherjee, J., M. D. Scharff, and A. Casadevall.** 1992. Protective murine monoclonal antibodies to *Cryptococcus neoformans*. Infect. Immun. **60:**4534–4541.
33. **Mukherjee, J., M. D. Scharff, and A. Casadevall.** 1994. *Cryptococcus neoformans* infection can elicit protective antibodies in mice. Can. J. Microbiol. **40:**888–892.
34. **Mukherjee, S., M. Feldmesser, and A. Casadevall.** 1996. J774 murine macrophage-like cell interactions with *Cryptococcus neoformans* in the presence and absence of opsonins. J. Infect. Dis. **173:**1222–1231.
35. **Near, R. I., R. Bruccoleri, J. Novotny, N. W. Hudson, A. White, and M. Mudgett-Hunter.** 1991. The specificity properties that distinguish members of a set of homologous anti-digoxin antibodies are controlled by H chain mutations. J. Immunol. **146:**627–633.
36. **Nosanchuk, J. D., and A. Casadevall.** 1997. Cellular charge of *Cryptococcus neoformans*: contributions from the capsular polysaccharide, melanin, and monoclonal antibody binding. Infect. Immun. **65:**1836–1841.
37. **Nosanchuk, J. D., W. Cleare, S. P. Franzot, and A. Casadevall.** 1999. Amphotericin B and fluconazole affect cellular charge, macrophage phagocytosis, and cellular morphology of *Cryptococcus neoformans* at subinhibitory concentrations. Antimicrob. Agents Chemother. **43:**233–239.
38. **Nussbaum, G., S. Anandasabapathy, J. Mukherjee, M. Fan, A. Casadevall, and M. D. Scharff.** 1999. Molecular and idiotypic analysis of the antibody response to *Cryptococcus neoformans* glucuronoxylomannan-protein conjugate vaccine in autoimmune and nonautoimmune mice. Infect. Immun. **67:** 4469–4476.
39. **Nussbaum, G., W. Cleare, A. Casadevall, M. D. Scharff, and P. Valadon.** 1997. Epitope location in the *Cryptococcus neoformans* capsule is a determinant of antibody efficacy. J. Exp. Med. **185:**685–697.
40. **Pirofski, L., R. Lui, M. DeShaw, A. B. Kressel, and Z. Zhong.** 1995. Analysis of human monoclonal antibodies elicited by vaccination with a *Cryptococcus neoformans* glucuronoxylomannan capsular polysaccharide vaccine. Infect. Immun. **63:**3005–3014.
41. **Richmond, D. V., and D. J. Fisher.** 1973. The electrophoretic mobility of microorganisms. Adv. Microb. Physiol. **9:**1–29.
42. **Sayle, R. A., and E. J. Milner-White.** 1995. RASMOL: biomolecular graphics for all. Trends Biochem. Sci. **20:**374.
43. **Valadon, P., G. Nussbaum, L. F. Boyd, D. H. Margulies, and M. D. Scharff.** 1996. Peptide libraries define the fine specificity of anti-polysaccharide antibodies to *Cryptococcus neoformans*. J. Mol. Biol. **261:**11–22.
44. **Valadon, P., G. Nussbaum, J. Oh, and M. D. Scharff.** 1998. Aspects of antigen mimicry revealed by immunization with a peptide mimetic of *Cryptococcus neoformans* polysaccharide. J. Immunol. **161:**1829–1836.
45. **Vargas-Madrazo, E., F. Lara-Ochoa, and J. C. Almagro.** 1995. Canonical structure repertoire of the antigen-binding site of immunoglobulins suggests strong geometrical restrictions associated to the mechanism of immune recognition. J. Mol. Biol. **254:**497–504.
46. **Vecchiarelli, A., and A. Casadevall.** 1998. Antibody-mediated effects against *Cryptococcus neoformans*: evidence for interdependency and collaboration between humoral and cellular immunity. Res. Immunol. **149:**321–333.
47. **Young, A. C. M., P. Valadon, A. Casadevall, M. D. Scharff, and J. C. Sacchettini.** 1997. The three-dimensional structures of a polysaccharide binding antibody to *Cryptococcus neoformans* and its complex with a peptide from a phage display library: implication for the identification of peptide mimotopes. J. Mol. Biol. **274:**622–634.
48. **Yuan, R., A. Casadevall, G. Spira, and M. D. Scharff.** 1995. Isotype switching from IgG3 to IgG1 converts a non-protective murine antibody to *C. neoformans* into a protective antibody. J. Immunol. **154:**1810–1816.
49. **Zhang, H., Z. Zhong, and L. Pirofski.** 1997. Peptide epitopes recognized by a human anticryptococcal glucuronoxylomannan antibody. Infect. Immun. **65:**1158–1164.

Editor: T. R. Kozel